IOSR Journal of Environmental Science, Toxicology and Food Technology (IOSR-JESTFT)
e-ISSN: 2319-2402,p- ISSN: 2319-2399.Volume 13, Issue 12 Ser. I (December. 2019), PP 51-60
www.iosrjournals.org

Dynamic Effects of Urban Heat Island in Ilaro Town, Yewa South LGA of Ogun, South West Nigeria

Adewara M.B [1], Oyewole A.M. [2]
1, 2 Department of Surveying & Geoinformatics, Federal Polytechnic Ilaro, Ogun State
Corresponding Author: Adewara M.B

Abstract: *There has been tremendous urbanization in the study area from 2000 to 2018. As a result of increasing construction activities there exists an increase in the number of floor plastering, dark colored roofs and buildings. These Pavements, dark-colored roofs, and similar surfaces absorb more sunlight, trap heat, and increase local temperatures. This research used satellite data (Landsat TM, ETM+ and OLI imageries acquired in 2000, 2010 and 2018) to examine the dynamic effect of Urban Heat Island in Ilaro town in Ogun state, Nigeria. Supervised classification algorithm in ENVI was used to classify the images into five land use /land cover classes (built up, bare lands, vegetation and cultivated/mixed vegetation). Landsat 8 OLI, Landsat 7ETM+ and Landsat 5 TM, were used for the LULC mapping and Land Surface Temperature analysis and the result showed that remote sensing images can be used to investigate how the LULC affects the surface temperature of the study area. The surface temperature of the different classes was recorded for each year and the urban thermal field variance index (UTFVI) was applied to measure the thermal comfort level of the city.The study established that there is a significant change in Land use pattern in area between 2000 and 2018, resulting in a gradual increasing rate in mean land surface temperature, LST (>5% per annum). This change in LULC pattern significantly increased the amount of heat emitted in the metropolis with more than 5^0C increase (9%). It is against this backdrop that proactive steps need be taken to control the menace of rapid rise in LST in Ilaro town, which includes afforestation, preservation of water bodies and reduction of the amount of bare surfaces.*

Keywords: *Classification, Land Surface Temperature (LST), Land Use/Land Cover (LULC), Satellite, Urbanization, Urban Heat Island (UHI), Urban Thermal Field Variance Index (UTFVI)*

Date of Submission: 28-11-2019 Date of Acceptance: 13-12-2019

I. Introduction

Ilaro, an urban town where the Yewa local government headquarter, Federal polytechnic Ilaro and center of economic activity is located has been attracting business people and student in the last few decades. The expansion of this urban area with the accompanying large population will require a larger area (Widya, 2017) as well as release more heat energy to its surroundings. This phenomena of increasing heat energy as a result of urbanization of the town is referred to as Urban Heat Island.

Heat Islands develop when a large fraction of the natural land cover in an area is replaced by built surfaces that trap incoming solar radiation during the day and then re-radiate it at night (Quattrochi, et al., 2000; Oke, 1982).

Urban Heat Island (UHI) is a phenomenon as "An Island" where the hot surface air is concentrated in urban areas and will progressively decrease in surrounding temperatures in suburban/rural areas (Widya, 2017). It is a phenomenon whereby urban regions experience warmer temperatures than their rural, undeveloped surroundings (Roth, 2013). As the urban area increases, there is increase in the use of manmade materials, at the same time anthropogenic heat production is on the increase, thus the main causes of UHI. This has led to the understanding that increased urbanization is the primary cause of the urban heat island (Abbas, Jason, & Tristan, 2017).

Higher temperatures attributed to the urban heat island effect increase the likelihood of oxides of nitrogen (NOx) and volatile organic compounds (VOCs) forming smog, which has serious health consequences. Ozone can inflame the respiratory tract and increase the lungs' susceptibility to infections, allergens, and other air pollutants.

Several other problems related to UHIs have been observed, such as increased urban pollution, intense summer rainfalls, and high energy consumption. Also, there may be problems related to thermal discomfort and heat stress impacting human health and causing a high death rate of already physically vulnerable people (Alves & Lopes, 2017).

UHI have effects on the quality of lives. These can be evaluated using a number of thermal comfort indices, some of which are the temperature humidity index (THI), the physiological equivalent temperature (Moser-Reischl, , et al., 2018), the wet-bulb globe temperature (WBGT), and the urban thermal field variance index (UTFVI) (Kakon, et al., 2010; Matzarakis, et al., 1999; Willett & Sherwood, 2012; Zhang, et al., 2006). Heat Islands of varying extent and magnitude have been observed in most urbanized areas in the world (Landsberg, 1981)

In this study, the trend of development of atmospheric UHI through changes in temperature and UHI index over time was explored and the impact of UHI on the quality of urban life in the area (from 2000 -2018) based on the UTVFI was evaluated using remote sensing and GIS.

Satellite data such as the Landsat with temporal, spatial and spectral characteristics affords us the opportunity to study the rise in temperature of the study area over different years (temporal resolution).

II. Materials And Method

2.1 Study area

Ilaro is situated on the rich cocoa belt of South Western Nigeria and with an above average rainfall. Geographically, Ilaro is bounded on the north by the Oyo Province on the South by Lagos and the east by the Egba division and on the west by Dahomey (Republic of Benin). The boundary on the South is defined in the "Colony of Nigeria boundaries order in council 1913. It lies between 496505.830mE, 763173.51mN and 496435.980mE, 759321.670mN. Ilaro town houses about 57,850 people, Ilaro town is the headquarters of the Yewa south Local government, now known as Yewa land. Ilaro town is about 50km from Abeokuta, Ogun state capital. Daily temperature of Ilaro town ranges between an average minimum 23 °C to a maximum of 34.2 °C. Farming is one major occupation of the dwellers of Ilaro town, they produce crops such as cocoa, coffee, kola-nuts, oranges, pineapples, cassava, yam, rice etc. Ilaro soils are mostly loamy and humus and rich in manure which supports of these crops. Also Ilaro dwellers (Yewa/Egbado people) produce timber, as a result of the thick forest in the town.

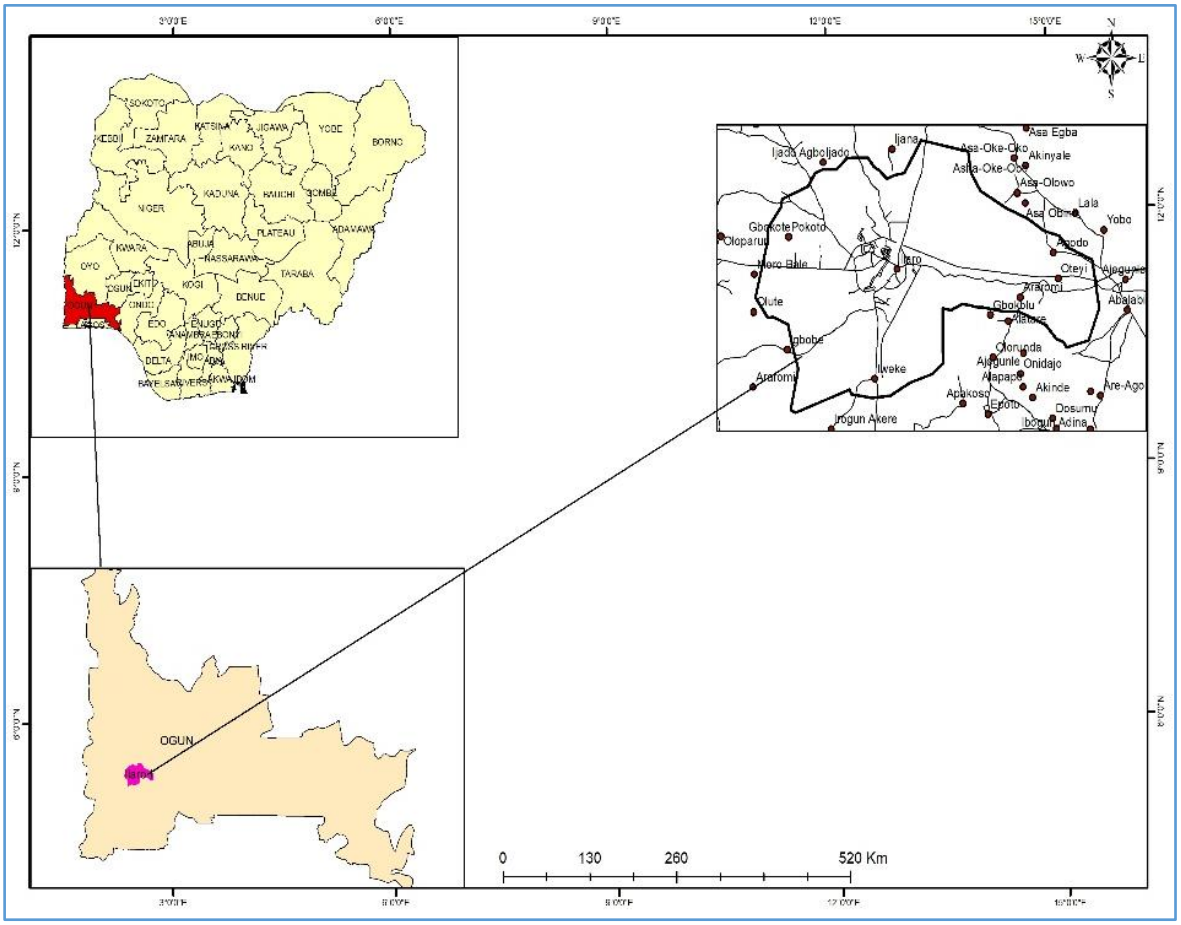

Figure 1: Map of the Study area

Flow chart

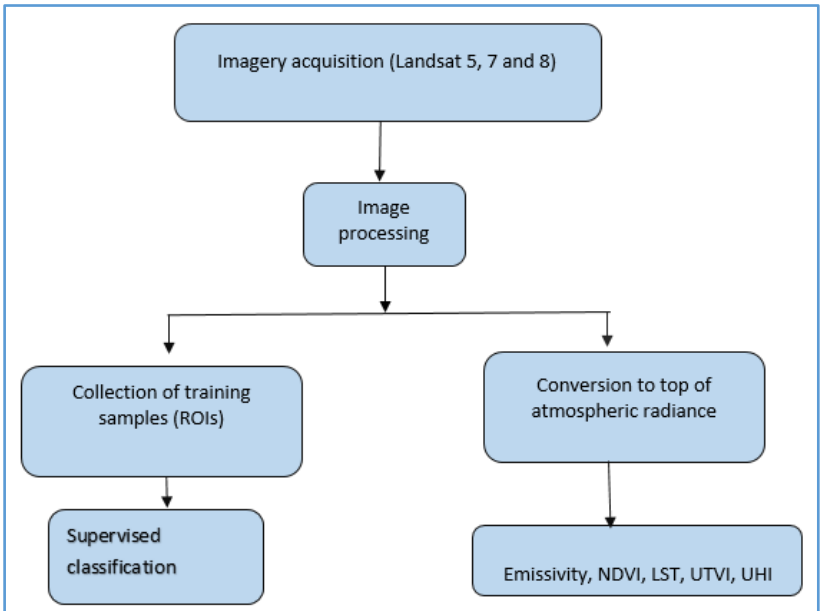

Figure 2: Flow process of the study

2.2 Materials

Remotely sensed imagery of Landsat TM, ETM and Landsat OLI imageries of 2000, 2010 and 2018 were used. Landsat TM with spatial resolution of 40 meters, Landsat ETM of spatial resolution of 30 meters and Landsat OLI of 28 meters' spatial resolution were used to detect the changes (table 1). The imageries were acquired in scenes from the USGS website. These datasets were all acquired in the dry season, to minimize cloud cover. Cloud cover inhibits perfect result, as the cloud would mask the real object on ground, and even affect the quality of the research procedure.

Table 1: Satellite Data Information

Satellite	Time	Path/Row	Bands used	Spatial resolution
Landsat 7 (Enhanced Thematic mapper)	November 2000, 2010	191/55	Visible bands:1,2,3 NIR: Band4, SWIR: Band 5, TIR: Band 6	30mx 30m
Landsat 8 Operational land imager/ thermal infrared sensor	November 2018	191/55	Visible bands:2,3,4 NIR: Band 5, SWIR: Band 6, 7,9 TIR:Bands10 and 11	30mx 30m

2.3 Methods

Despite that the remotely sensed imageries have been corrected for radiometric and geometric distortion, however, some errors need to be corrected by the user, such as cloud removal or reduction, line dropout removal etc. some of the Landsat 7 dataset have line dropout errors which were corrected in this study, for better accuracy. Several image processing techniques were applied to enhance visual perception; composite bands, sub-setting, layer stack etc.This image processing helped in image interpretation, which is an important aspect while performing supervised image classification algorithm.

2.4 Land Use Land Cover Classification

The supervised image classification method was adopted in this study using the ENVI 5.3 classic software. This method uses the spectral signature that is defined in the training set by determining each class on what it resembles most in the training set.

Regions of interests, ROI were created and were used as training sites to classify the imagery. The maximum likelihood classification algorithm was used.

$$g_i(x) = \ln p(\omega_i) - {}^1/_2 \ln |\sum_i| - {}^1/_2 (x - m_i)^T \sum_i^{-1} (x - m_i)$$ (Richards, 1999)

Where

i = class

x = n-dimensional data (where n is the number of bands)

$p(\omega_i)$ = probability that class ω_i occurs in the image and is assumed the same for all classes

$|\Sigma_i|$ = determinant of the covariance matrix of the data in class ω_i
Σ_i^{-1} = its inverse matrix
m_i = mean vector

This is because this algorithm assumes that the statistics for each class in each band are normally distributed and calculates the probability that a given pixel belongs to a specific class. Four (4) land cover classes were identified in the study area; Bare surface/soil, Riperian vegetation or thick vegetation (forest), Light vegetation and Built up.

Table 2: Land Use land Cover types in the study area

	LULC	**Description**
1	Urban built- up area	Includes areas with all types of artificial surfaces, including residential, commercial, and industrial land uses as well as transportation infrastructure
2	Bare surface/bare soil	Cultivated land, cleared land
3	Thick vegetation(forest/riparian vegetation)	Includes areas with dense vegetation cover, such as those covered with shrubs forming closed canopies, trees and other vegetation that is relatively tall and dense, as well as areas covered with both indigenous and exotic trees
4	Light vegetation	Grasslands and shrubs

III. Results and Discussion

3.1 Change in Land Use Land Cover

Land use documents how people are using the land whereas Land cover indicates the physical land type such as forest or open water. The Land Use land Cover maps of the area were produced for the years under study.

For the purpose of validating the result of the image classification, we compared the classification output with ground truth data to determine the classification accuracy. This technique is called accuracy assessment. Based on the LU/LC cover classification technique used, a temporal land use and land cover change between the year 2000 and 2018, was prepared using the cross tabulation technique. This was done using the ENVI 5.3 classic software, by selecting the post classification tab. The cross tabulation method overlays newer classified image on older images, to produce the changes and loses between the two images.

Table 3: Cross tabulation for LU/LC between 2000 and 2010

Area in (Square Km)	**LU/LC 2000 - 2010**					
	Built Up	Thick forest/Riparian vegetation	Light vegetation	Bare Surface	Row Total	Class Total
Built Up	3.99	0	0	0	3.99	3.99
Vegetation	0	166.77	0	0	166.77	166.77
Riparian Vegetation	0	0	45.76	0	45.76	45.76
Bare surface	0	0	0	41.08	41.08	41.08
Class Total	3.99	166.77	45.76	41.08	0	0
Class Changes	0	166.77	45.76	41.08	0	0
Image Difference	0	-121.01	-4.68	125.69	0	0

Table 4: Cross tabulation for LU/LC between 2010 and 2018

Area in (Square Km)	**LU/LC 2010 - 2018**					
	Built Up	Thick forest/Riparian vegetation	Light vegetation	Bare Surface	Row Total	Class Total
Built Up	0	0	0	0	0	0
Vegetation	126.05	0	0	0	126.05	126.05
Riparian Vegetation	0	51.19	0	0	51.19	51.19
Bare surface	0	0	59.75	0	59.75	59.75
Class Total	0	0	0	20.6	20.6	20.6
Class Changes	126.05	51.19	59.75	20.6	0	0
Image Difference	0	0	0	0	0	0

3.2 Accuracy Assessment

To assess the obtained accuracy of the Land Use Land cover classification, a comparison of the relationship between known reference data (ground truth) and the corresponding results of the classification procedure was performed using the a confusion matrix. Accuracy assessment was obtained for each year from 2000, 2010, and 2018. This calculated from the Kappa coefficient which is given as:

$$K = \frac{N\sum_{i=1}^{r} x_{ii} - \sum_{i=1}^{r}(x_i + Xx_{+1})}{N^2 - \sum_{i=1}^{r}(x_{ii} Xx_{+1})}$$

(Adam, 2011)

Where:

r = Number of rows/columns in confusion matrix
Xii = Number of observation in row i and column i
Xi+ =Total number of row i
X+I = Total number of column i
N = Number of observations

The overall classification accuracy is obtained by dividing the total number of correctly classified samples by the total number of reference samples. It is the percentage of correctly classified samples of an error matrix. It is calculated using equation:

$$\text{Overall accuracy} = \frac{1}{N}\sum_{k-1}^{n} a_{kk}$$

(Banko, 1998)

Accuracy Assessment for 2000

Confusion Matrix: 2000
Overall Accuracy = (392/408) = 96.0784%
Kappa Coefficient = 0.9178

Table 5: Accuracy Assessment for 2000

	Ground Truth (Percent)			
Class	Built Up	Riparian Vegetation	Bare surface	Total
Built Up (Red)	100	0.00	13.33	12.01
Riparian Vegetation	0.00	98.58	0.00	67.89
Bare surface	0.00	1.42	86.67	20.10
Total	100.00	100.00	100.00	100.00

Accuracy Assessment for 2010

Confusion Matrix: 2010
Overall Accuracy = (640/661) = 96.8230%
Kappa Coefficient = 0.9544

Table 6: Accuracy Assessment for 2010

Class	**Commission (%)**	**Omission (%)**	**Commission** (Pixels)	**Omission** (Pixels)
Built up (Red)	0.00	3.41	0/85	3/88
Bare Surface	4.29	1.27	7/163	2/158
Light Vegetation	2.78	3.11	8/288	9/289
Riparian Vegetation/thick vegetation	4.80	5.56	6/125	7/126

Accuracy Assessment for 2018

Confusion Matrix: 2018
Overall Accuracy = (539/549) = 98.1785%
Kappa Coefficient = 0.9724

Table 7: Accuracy Assessment for 2018

Class	**Commission(%)**	**Omission (%)**	**Commission** (Pixels)	**Omission** (Pixels)
Built Up (Red)	0.47	0.94	1/211	2/212
Bare surface	2.38	1.20	2/84	1/83
Light vegetation	20.59	0.00	7/34	0/27
Riparian Vegetation/thick vegetation	0.00	3.08	0/220	7/227

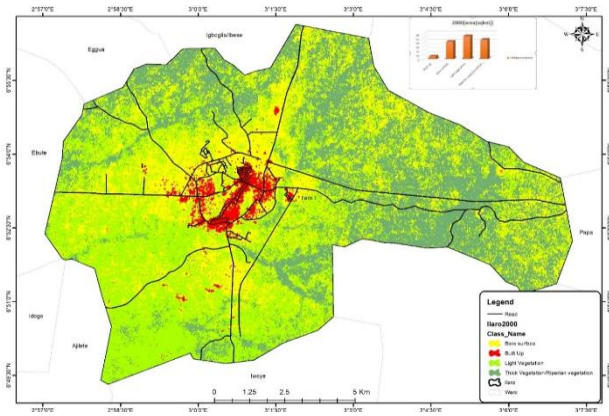

Figure 3: Land Use Land cover in 2000

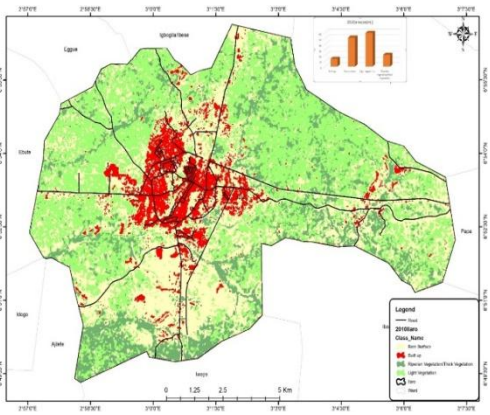

Figure 4: Land Use Land cover in 2010

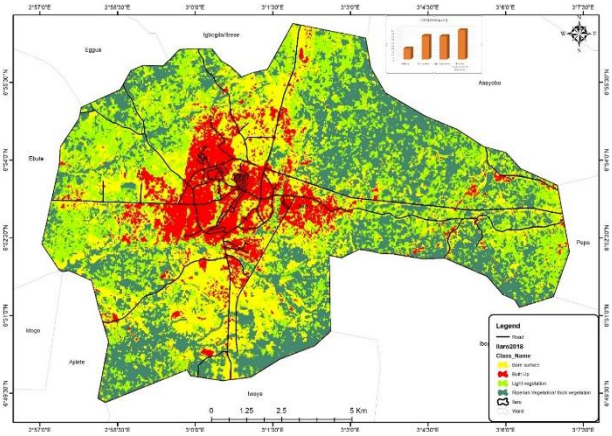

Figure 5: Land Use Land cover in 2018

The maps above show the changes that occurred in Ilaro town between 2000 and 2018. The changes are summarizedin terms of coverage areas (table8 and figure 6).

Table 8: Coverage area of each Land Use / Land Cover class for each year.

Land use/Land cover type	**2000 (Km^2)**	**2010 (Km^2)**	**2018 (Km^2)**	**% increase/decrease**
Built up	5.763718	13.69881	18.173086	32.97
Bare Surface	41.048254	51.125829	39.185914	1.40
Light vegetation	54.33862	59.66458	38.880049	10.11
Riparian vegetation/thick vegetation	45.669132	20.554634	48.804874	2.73

Between 2000 and 2018 there is an increase in the coverage area of the built up areas by 32.97% while bare surface, light vegetation and thick vegetation reduced by 1.40%, 10.11% and 2.73% respectively. This implied that the built up area had tripled. The bare surface and the vegetative areas are closing up in sizes due to urbanization. Most of the thick vegetation cover have been reduced to light or thin vegetation and most of the light vegetation have metamorphosed to bare soil and built up areas.

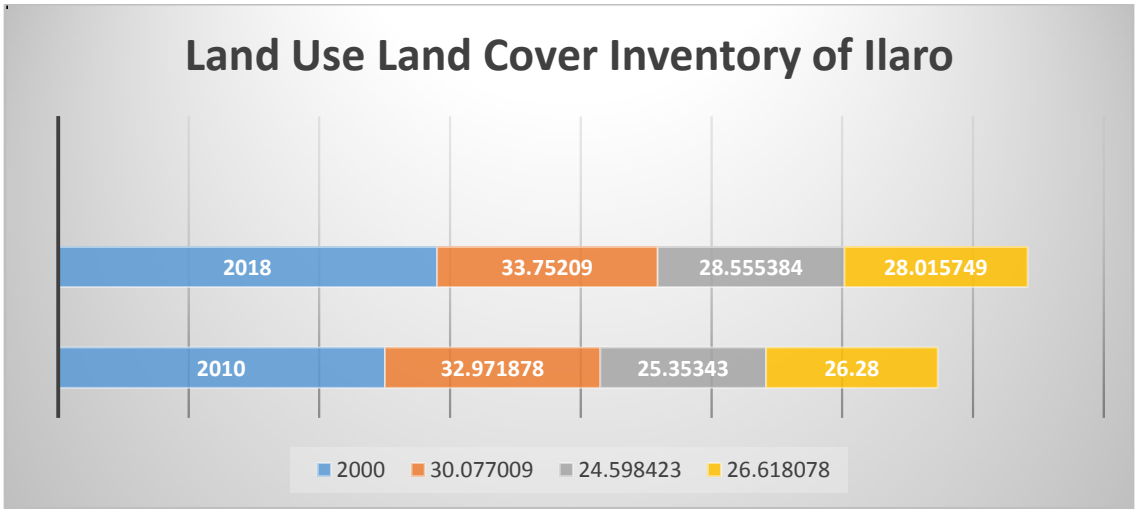

Figure 6: Land Use Land Cover Inventory of the study Area

3.3 Land-Use/Land Cover (LULC) based on Land Surface Temperature (LST)

LST is one of the most important environmental parameters used in determining the exchange of energy and matter between the surface of the earth and the lower layer of the atmosphere. It shows how hot the surface of a place would feel to touch. Figures 7 - 9 show the maximum and minimum land surface temperatures between 2000 and 2018 and table 11 show the changes in the Land surface temperature for the different LU/LC.

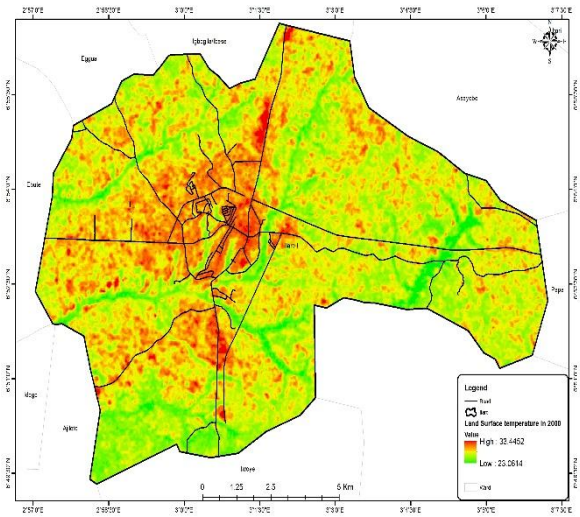

Figure 7: LST distribution in 2000

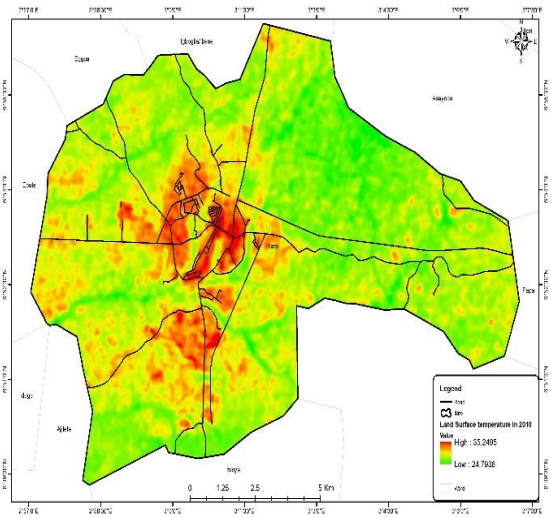

Figure 8: LST distribution in 2010

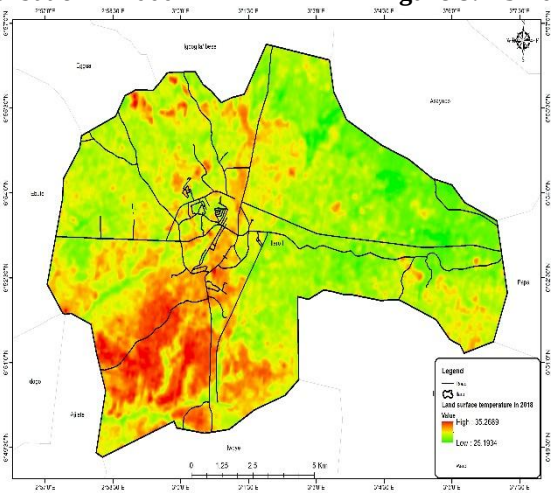

Figure 9: LST distribution in 2018

Table 9: Changes in the Land Surface Temperature

	Land Surface Temperature (LST)		
Land Use/Land Cover (LULC)	**2000**	**2010**	**2018**
Built Up	30.077009	32.971878	33.75209
Riparian/ thick forest	24.598423	25.35343	28.555384
Light vegetation	26.618078	26.28	28.015749
Bare surface/soil	29.588655	31.900617	31.664524

Between 2000 and 2018 the land surface temperature of the built up area has increased. 2018, in fact, was the year with the highest land surface temperatures over the area. Generally, over the years, the land surface temperatures of the land use land cover types have been on the increase. There is the likelihood that the increase will continue to the nearest years. This is attributable to the increasing urbanization and decreasing vegetation cover. As the built up areas& bare surfaces increase, there is adverse reduction in green cover. This has direct impact on the last surface temperature of the area (figure 10).

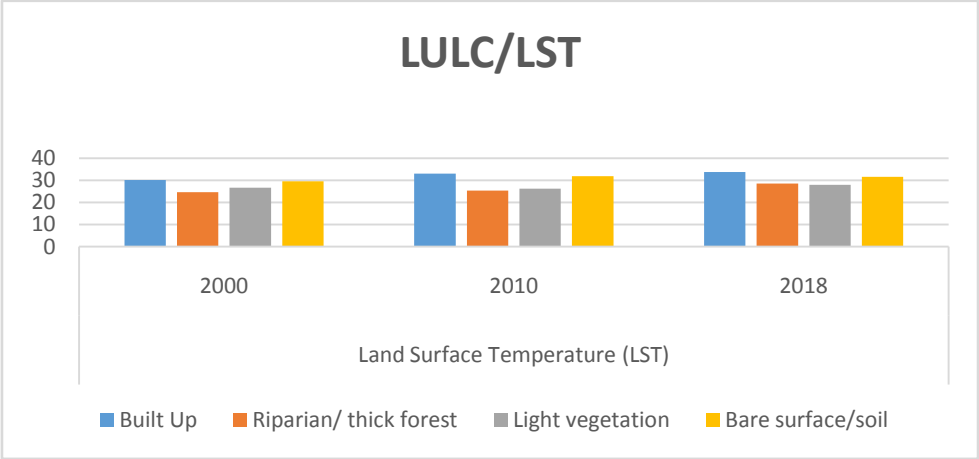

Figure 10: Changes in LST with changing LULC type.

3.3.1 Urban Thermal Field Variance Index (UTFVI), Urban Heat-Island (UHI) Effect and Ecological Conditions from the LST of Ilaro town

It was observed that the vegetation and water body areas which act as heat sink have relatively lower temperatures. The densification of the vegetation lowers the temperature as it enhances the evapotranspiration that maintains the heat flux (Joshi & Bhatt, 2012). The thermal and ecological comfort level of the city was determined using the urban thermal field variance index (UTFVI).Several urban heat islands (UHIs) were extracted as the most heated zones within the city boundaries due to increasing anthropogenic activities. The urban thermal field variance index is commonly used to express the urban heat island effect. It can be calculated by

$$UTVI = \frac{T_S - T_{mean}}{T_S}$$ (Zhang, et al., 2006)

where T_s = LST in certain point of the map

T_{mean} = the corresponding mean temperature of the whole town.

UTFVI = Urban Thermal Field Variance Index;

LST = surface temperature of certain point in °C (temperature of points in a certain Land use or land cover type),

The result of UTVI is classified into six (6) classes where each class corresponds to the ecological index. This is to be able to illustrate the level of urban heat island effectively.

Table 10: Urban Heat Island Intensity Classification Index

Urban Thermal Field Variance Index (UTFVI)	Urban Heat Island Phenomenon (UHI)	Ecological Evaluation Index (EEI)
<0	None	Excellent
0.000–0.005	Weak	Good
0.005–0.010	Middle	Normal
0.010–0.015	Strong	Bad
0.015–0.020	Stronger	Worse
> 0.020	Strongest	Worst

Table 11: UTFVI for the study area between 2000 and 2018

UTVI (2000)	UTVI (2010)	UTVI (2018)
11.1519869	7.027437201	7.702281332
-8.8433371	-8.663189331	-35.05379713
-34.935437	-13.14	-20.68726477
13.3966849	8.810823404	13.80004044

Throughout the study years, thick forest and light vegetation zones had the best ecological index while built up and bare surfaces has the worst. The correlation between each land use land cover class, with the Urban Thermal field variance index (UTFVI) and the corresponding ecological conditions for each value for the study area is shown in table 11-14.The tables showed that the thick forest and light vegetation zones had the best ecological index throughout the study years while built up and bare surfaces has the worst. The implication of this is that there has been rapid urbanization from 2000 till 2018 as a result of influx of migrants into the town for job, businesses and educational purposes. The settlement of migrants and students thus increased demand for housing and infrastructure in the areathereby increasing the built up and bare surface areas.

Table 12: LULC, UTVI and Ecological Conditions from the LST of the study area in 2000

Land Use/Land Cover	UTVI(2000)	UHI PHENOMENON	Ecological index
Built Up	11.1519869	strongest	Worst
Riparian/ thick forest	-8.8433371	None	Excellent
Light vegetation	-34.935437	None	Excellent
Bare surface/soil	13.3966849	strongest	worst

Table 13: LULC, UTVI and Ecological Conditions from the LST of the study area in 2010

Land Use/land Cover	UTVI(2010)	UHI PHENOMENON	Ecological index
Built Up	7.027437201	strongest	Worst
Riparian/ thick forest	-8.663189331	None	Excellent
Light vegetation	-13.14	None	Excellent
Bare surface/soil	8.810823404	strongest	worst

Table 14: LULC, UTVI and Ecological Conditions from the LST of the study area in 2018

Land Use/Land Cover	UTVI(2018)	UHI PHENOMENON	Ecological index
Built Up	7.702281332	strongest	Worst
Riparian/ thick forest	-35.05379713	None	Excellent
Light vegetation	-20.68726477	None	Excellent
Bare surface/soil	13.80004044	strongest	worst

IV. Conclusion And Recommendation

Generally, throughout the study period, there has been a subsequent increase in land surface temperature across the different land use and land cover types in the study area as a result of urbanization. Built ups and Bare surfaces or bare soil now accounts for a very integral figure in the total land use or land cover of the town. Land surface temperature shows an increasing trend in built up areas and bare surfaces. The study had an overall classification accuracy of 97.03% and kappa coefficient of 0.948. The kappa coefficient is rated as substantial and hence the classified image found to be fit for further research.

The trend in land use changes in the area has visible environmental impacts on the surrounding natural resources and the ecosystems. Dark roofs and pavements absorb heat from the sunlight and make houses and surroundings warm. In contrast, light colored roofs with similar insulation properties do not get warmed significantly by reflecting solar radiation (Akbari, Pomerantz, & Taha, 2001). This means that the choice of roofing color can contribute to temperature reduction. Therefore, to improve the thermal environment around buildings and pavements and mitigate UHI, it is suggested to use the material of lower absorptivity, higher reflectivity, and larger thermal conductivity (Xu, Bruelisauer, & Berger, 2017).

One of the most effective strategies to mitigate UHI in the study area is to increase the size of green/vegetative areas by tree planting trees. Trees planting reduces the heat island effect by their evapotranspiration (Akbari, Pomerantz, & Taha, 2001).

This paper have also demonstrated that the cut-edge technology of remote sensing for environmental changes research gives it an edge over in-situ techniques.

Acknowledgement

The authors wish to the support of Tertiary Education Trust Fund (TETFund) for awarding the research grant through the Federal Polytechnic, Ilaro that give an enabling environment to execute the research. All the authors whose previous work and published data have contributed to the present study are acknowledged, and so are the efforts of the reviewers of this paper.

Reference

[1]. Abbas, M., Jason, B., & Tristan, J. B. (2017). The urban heat island effect, its causes, and mitigation, with reference to the thermal properties of asphalt concrete. Journal of Environmental Management, 522-538.

[2]. Abu Bakar, S. B., Pradhan, B., Usman , S. L., & Abdullahi , S. (2016). Spatial assessment of land surface temperatureand land use/land cover in Langkawi Island. 8th IGRSM International Conference and Exhibition on Remote Sensing & GIS (IGRSM 2016). Selangor: IOP.

[3]. Abu Yousuf, M. A., Arif , M., Mohammed, S. G., Md. Abdullah , A., Quazi , K. H., & Ashraf , D. (2019). Spatio-Temporal Patterns of Land Use/Land Cover Change in the Heterogeneous Coastal Region of Bangladesh between 1990 and 2017. Remote Sensing, 2.

[4]. Adam, H. E. (2011). Integration of Remote Sensing and GIS in Studying Vegetation Trends and Conditions in the Gum Arabic Belt in North Kordofan, Sudan, PhD thesis. TU Dresden, Germany.

[5]. Akbari, H., Pomerantz, M., & Taha, H. (2001). Cool surfaces and shade trees to reduce energy use and improve air quality in urban areas. Journal of Solar energy, 295-310.

[6]. Alves, E. D., & Lopes, A. (2017). The Urban Heat Island Effect and the Role of Vegetation to Address the Negative Impacts of Local Climate Changes in a Small Brazilian City. Journal of Atmosphere , 2-14.

[7]. Banko, G. (1998). A Review of Assessing the Accuracy of Classifications of Remotely Sensed Data and of Methods Including Remote Sensing Data in Forest Inventory. A-2361 Laxenburg. Austria : International Institute for Applied Systems Analysis.

[8]. Effat, H. A., & Hassan, O. A. (2014). Change detection of urban heat islands and some related parameters using multi-temporal Landsat images; a case study for Cairo city, Egypt. Urban Clim, 171–88.

[9]. Joshi, J. P., & Bhatt, B. (2012). Estimating temporal land surface temperature using remote sensing: a study of vadodara urban, Gujarat. International Journal of Geology, Earth and Environmental Sciences, 123–130.

[10]. Kassahun, G., & Tegegne , G. E. (2018). Spatiotemporal trends of urban land use/land cover and green infrastructure change in two Ethiopian cities: Bahir Dar and Hawassa. Environmental Systems Research, 1.

[11]. Landsberg, H. E. (1981). The Urban Climate. New York: National Academy Press.

[12]. Laura , B., Tobias, R., Martin , B., Marta Díaz-Zorita , B., Philipp , G., Karsten , S., & Thomas, S. (2019). Analysisandmappingofspatio-temporal land use dynamics in Andalusia, Spain using the Google Earth Engine cloud computing platform and the Landsat archive. Geophysical Research, 1.

[13]. Lu, D., & Weng, Q. (2007). A survey of image classification methods and techniques for improving classification performance. International Journal of Remote Sensing, 823-870.

[14]. Moser-Reischl, , A., Uhl, E., Rötzer, T., Biber, P., Van Con, T., Tan, N. T., & Pretzsch, H. (2018). Effects of the urban heat island and climate change on the growth of Khaya senegalensis in Hanoi, Vietnam. Forest Ecosystem, 37.

[15]. Oke, T. R. (1982). The Energetic Basis of Urban Heat Island. Journal of the Royal Meteorological Society, 1-24.

[16]. Quattrochi, D., Luvall, J., Rickman, D., Estes, M., Laymon, C., & Howell, B. (2000). A decision supportinformation system for urban landscapemanagement using thermal infrared data.Photogrammetric Engineering and RemoteSensing. 66 (10), . Journal of Photogrammetric Engineering and RemoteSensing, 1195-1207.

[17]. Richards, J. (1999). Remote Sensing Digital Image Analysis. Berlin: Springer-Verlag.

[18]. Roth, M. (2013). Urban Heat Islands. In J. S. Harindra, Handbook of Environmental Fluid Dynamics (pp. 143-158). Singapore: Taylor & Francis Group.

[19]. Tokairin, T., Sofyan , A., & Kitada, T. (2010). Effect of land use changes on local meteorological conditions in Jakarta, Indonesia: Toward the evaluation of the thermal environment of megacities in Asia. International Journal of Climatology, 1931–41.

[20]. Vahid, A. P., & Esmail, S. (2016). Spatio-temporal analysis and simulation pattern of land use/cover changes, case study: Naghadeh, Iran. Journal of Urban Managemen, 43.

[21]. Widya, N. (2017). Urban Heat Island towards Urban Climate. Global Colloquium on GeoSciences and Engineering, 1-6.

[22]. Xu, M., Bruelisauer, M., & Berger, M. (2017). Development of a new Urban Heat Island Modeling Tool : Kent Vale case study. Amsterdam: Elsevier.

[23]. Zhang, Y., Yu, T., Gu, X., Zhang, Y., Chen, L., Yu, S., . . . Li, X. (2006). Land surface temperature retrieval from CBERS-02 IRMSS thermal infrared data and its applications in quantitative analysis of urban heat island effect. Journal of Remote Sensing-Beijing, 10-17.

Adewara M.B "Dynamic Effects of Urban Heat Island in Ilaro Town, Yewa South LGA of Ogun, South West Nigeria" IOSR Journal of Environmental Science, Toxicology and Food Technology (IOSR-JESTFT) 13.12 (2019): 51-60.